Control of Robotic Crawler Cranes in Tandem Lifting Operations

Sima Rishmawi
Department of Mechanical and
Mechatronics Engineering
Birzeit University
PO Box 14, Birzeit, West Bank, Palestine
Email: srishmawi@birzeit.edu

William Singhose
Woodruff School of Mechanical Engineering
Georgia Institute of Technology
Atlanta, GA, 30332, USA
Email: singhose@gatech.edu

***Abstract*—Moving heavy and over-sized loads poses significant control challenges. A single crawler crane may be insufficient for such lifting tasks if the payload exceeds the capacity, or if the payload's size and shape make it difficult to secure it to a single crane hook. To solve these problems, it may be necessary to manipulate such items by tandem lifting with two cranes. These cranes are usually driven by two operators whose actions are coordinated by a lift director. In this paper, a pseudo-dynamic model describing the behavior of such a system, when the bases of the cranes are moving in a straight line, is derived. The paper also sets basic guidelines that prevent tip-over accidents. Finally, it presents a control system that eliminates the need for a second crane operator by making one crane mimic the behavior of the other crane, thus reducing the possibility of human errors.**

***Keywords*—Crawler; crane; tandem; robotic; tip-over stability; control; crane safety**

I. Introduction

Modern industrialization is driving the need for heavy cargo manipulation. This includes the components used in renewable and sustainable energy developments, such as tall wind turbines. Wind turbine components are an excellent illustration of large cargo that pose significant challenges due to their considerable mass and size. The machinery housings, called nacelles, are very heavy, while the rotor blades are extremely bulky and awkward to manipulate [1].

Pre-cast concrete yards are another example of an environment where lifting huge and bulky loads is a critical challenge that needs to be tackled with utmost care. Pre-cast concrete elements are usually constructed offsite, thus one of the major operations that need to be executed is the transportation of such elements to and around the construction site. The difficulty lies in the fact that some pre-cast concrete lifts cannot be achieved using single cranes or conventional lifting methods [2].

In order to address challenges resulting from huge or awkwardly shaped objects, tandem lifting is suggested as an alternative method of lifting to single-crane lifts. Tandem lifting implies that two or more cranes are used to lift one common payload that is attached to each of the cranes' hooks. Such a case is shown in Fig. 1.

Unless it is the only possible solution, tandem lifting is usually avoided. Tandem lifts present greater safety risks than single-crane lifts. One safety risk involves synchronizing the movement of both cranes. Lateral forces acting on the crane boom have to be prevented, in addition to overloads, side loads, unequal load sharing, and overturning moments. Hoisting at unequal speeds, for example, can result in unequal load distribution. This scenario can lead to an overload on one of the cranes.

Fig. 1. Tandem-lifting cranes [3].

The two cranes involved in tandem lifting are operated by two crane operators; therefore, synchronizing human operator actions comes into play. This implies the need of a third person (lift director) to coordinate the actions of both crane operators. It should be noted that even if the operators perform flawlessly, it is still impossible to synchronize the cranes' movement perfectly. Therefore, additional safety measures should be utilized and appropriate control systems should be developed [1].

To mitigate hazards, ISO standard 12480-1 suggests that all lateral forces on the crane boom have to be avoided and the crane movements have to be synchronous. Furthermore, a crane is allowed to lift 100% of the load suggested in its load chart, only if all relevant factors can be monitored. If one or more of the factors cannot be evaluated, then the load weight must be down-rated by 25% or more, depending on the situation. Thus, it should be understood that for almost every advantage gained by using tandem-lifting cranes, there is a disadvantage to consider [1].

There have been several investigations of the tip-over

stability of cranes in single and tandem lifting. For example, Neitzel et al. [4] reviewed available information on crane-related injuries, and gave recommendations for improving crane injury prevention and future crane safety research. The tip-over stability of a mobile crane considering the payload oscillations was investigated by Rauch et al. [5]. The comparison between static stability and the full dynamic stability revealed that a simple semi-dynamic analysis provides good approximations for the tip-over stability properties.

Payload swing has a significant influence on the stability of cranes. A combined feedback and input shaping controller was developed in [6]. This controller, which is comprised of three distinct modules, was able to reduce payload swing and achieve good positioning. It was successfully implemented on a $10-$ton bridge crane at the Georgia Institute of Technology.

The payload and the hoisting cable of an overhead crane were modeled as a double pendulum in [7]. Also, a double pendulum with two fixed-length links and a kinematic constraint model was developed for quay-side container cranes to obtain a nonlinear approximation of the oscillation frequency of a simplified model in [8], [9]. A two-degree of freedom mathematical model based on the physical structure of the crane's spreader was also used to describe a container crane spreader's dynamics in [10].

In [11], the payload swing caused by base excitation was investigated and limited by using reeling and unreeling of the hoisting cable. The payload was modeled as a point mass, the cable was modeled as a rigid link, and the assembly was attached to the boom tip. An excitation was applied to the assembly at the boom tip. The motion of the payload was described using two-dimensional and three-dimensional models. Shaping the commands has proven to be an effective method of reducing payload swing [12], [13], [14].

The idea of automated crane operations was previously studied and discussed. Shinde presented some tools required to implement automated robotic crane processes in [15]. Also in [16], Saidi et al. were able to develop a robotic crane for automated steel construction (RoboCrane), thus achieving autonomous placement of a steel beam.

In [17], construction cranes are treated as multi-degree-of-freedom robots modeled in a virtual environment. Virtual cranes are provided with algorithms to help plan their motions. Inverse kinematics are then used to determine the crane motions required to follow the computed paths.

Finally, an automatic cooperative hoisting system is developed in [18]. Using this system, an object can be lifted cooperatively using two cranes without the guidance of a lift director.

This paper presents a pseudo-dynamic linear model of two crawler cranes in tandem lifting. At first, payload oscillations induced by straight-base motion are investigated. Two controllers are then developed; the first aims at reducing these oscillations to a minimum value by use of command shaping, and the second aims at sensing the motion commands given by a human operator driving one of those cranes, and using them to actuate the other crane in perfect synchronization, thus minimizing the possibility of human error.

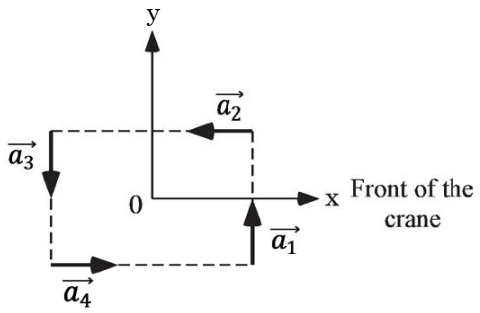

Fig. 2. Top view of the horizontal plane formed by the possible tip-over axes.

II. Tip-Over Stability based on the Sum of Moments about the Forward Tip-Over Axis

In this section, tip-over stability is investigated. The moment created by each gravitational force about a corresponding tip-over axis is calculated. In order to maintain stability, the sum of these moments, about each possible tip-over axis, should be less than or equal to zero.

It should be noted that crawler cranes move at very slow speeds. Furthermore, when the payload swings out, it oscillates with very low frequencies. Considering these facts, in addition to the huge masses of the crane components, it can be safely assumed that when the suspension cable is deflected by the swinging payload, it remains fixed in the maximum deflected position for a significant period of time. This assumption allows the use of static equations to calculate the sum of moments about the tip-over axis, thus minimizing the computational cost to predict tip-over stability. However, one should keep in mind that the maximum payload swing out angle is calculated from the pseudo-dynamic mathematical model explained in the following section.

Fig. 2 shows the general geometry of the possible tip-over axes of a crawler crane. The possible tip-over axes run along the front and rear edges, as well as the outside edges of the crawler tracks. Vectors $\vec{a_1}$ and $\vec{a_3}$ represent the forward and backward tip-over axes respectively, while $\vec{a_2}$ and $\vec{a_4}$ represent the sideway tip-over axes. In this paper, we are concerned with the case of tipping over the forward axis when the payload swing angle exceeds its allowed limit.

Fig. 3 illustrates the static forces acting on two crawler cranes in tandem lifting, where the payload is swinging. For simplicity, the two cranes are identical, with equal hoist cable lengths to ensure that the payload stays level throughout the whole process, which is recommended in such operations.

Each crane consists of a mobile base, m_1, a rotational boom, m_2, a counterweight, m_3, and a suspension cable with a payload mass, m_4 that is shared between both cranes. The base is modeled as a thin plate and has a center of gravity at the center of the base. The boom has a length of L_2. Its center of mass is located at the middle of the boom. The boom is elevated at an angle ϕ relative to the horizontal plane. This angle is known as the luffing, or boom, angle. The boom base is located at the center of the base for simplicity. The position of the counterweight is measured by a distance, L_3,

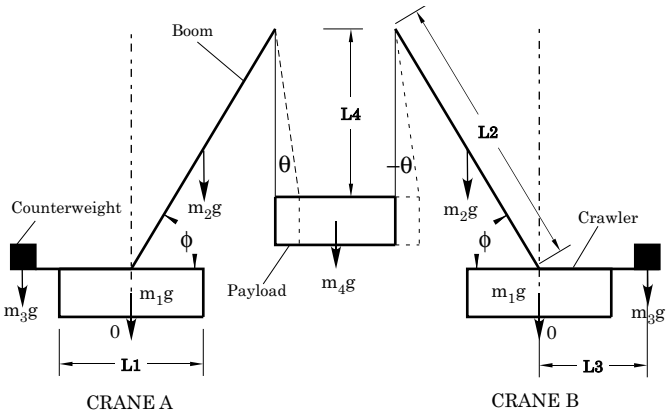

Fig. 3. Schematic diagram for tandem crawler cranes (load is shown in a swung-out position).

from the central axis. The payload swing angle, measured from the vertical is θ.

To calculate the moment generated by each of the gravitational forces about a given axis we use:

$$\vec{M_{ij}} = \vec{a_j} \cdot (\vec{r_i} \times \vec{f_i}) \tag{1}$$

where: $i = 1, ..., 4$ and $j = 1, ..., 4$.

$\vec{M_{ij}}$ is the moment generated by the force $\vec{f_i}$ about the axis $\vec{a_j}$ $[Nm]$.

$\vec{f_i}$ is the gravitational force acting on body i at its gravitational center $[N]$.

$\vec{a_j}$ is a unit vector along the j^{th} tip-over axis.

$\vec{r_i}$ is a position vector pointing from any point on the tip-over axis to any point on the line of action of the force $\vec{f_i}$ $[m]$.

The individual moments found using (1) are combined to produce the total moment about each tip-over axis:

$$\vec{M_j} = \sum_{i=1}^{4} \vec{M_{ij}} = \sum_{i=1}^{4} \vec{a_j} \cdot (\vec{r_i} \times \vec{f_i}) \tag{2}$$

Fig. 4 shows the forces acting on the payload in the swinging position. The reactions of these forces act on Cranes A and B and should be used in the moment equation in addition to the gravitational forces. Where:

$$\vec{F_1} = \frac{m_4}{2} g \tag{3}$$

$$\vec{F_2} = \frac{m_4}{2} g \tan\theta \tag{4}$$

Therefore, the moment creating a forward tip-over for Crane A is:

$$\vec{M_{fA}} = m_2 g(\frac{L_2}{2}\cos\phi - \frac{L_1}{2}) - m_1 g \frac{L_1}{2} - m_3 g(L_3 + \frac{L_1}{2}) + \frac{m_4}{2} g(L_2 \cos\phi - \frac{L_1}{2}) + \frac{m_4}{2} g \tan\theta (L_2 \sin\phi + h) \tag{5}$$

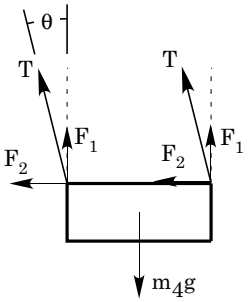

Fig. 4. Free body diagram of the payload.

And the moment creating a forward tip-over for Crane B is:

$$\vec{M_{fB}} = m_2 g(\frac{L_2}{2}\cos\phi - \frac{L_1}{2}) - m_1 g \frac{L_1}{2} - m_3 g(L_3 + \frac{L_1}{2}) + \frac{m_4}{2} g(L_2 \cos\phi + \frac{L_1}{2}) - \frac{m_4}{2} g \tan\theta (L_2 \sin\phi + h) \tag{6}$$

Equations (5) and (6) assume that the payload is swung outward from Crane A and inward toward Crane B.

III. Pseudo-Dynamic Model

When two crawler cranes are used in tandem lifting, they may have to be moved. Therefore, it is essential to study the effects of different motions on the tandem crane system stability. One of the main dynamic effects that needs to be considered is payload swing. This paper will focus on one of the major motion types that induce payload swinging: straight-base motion.

Generally, in the case of two cranes performing tandem lifting, the payload actually rotates with three different angles: θ_1 which represents the swing angle of the hoist cable connecting the payload to Crane A, θ_2 which represents the swing angle of the hoist cable connecting the payload to Crane B, both measured with respect to the vertical axis, and finally, θ_3 which represents the rotation angle of the payload about its center of gravity, measured with respect to the horizontal axis.

Because one of the goals of this paper is to develop a simple tool that requires minimal computational effort to predict the tip-over stability of the crawler cranes, the two cranes used are identical with equal hoist lengths. This assumption ensures that the payload stays level during operation (which is highly recommended), thus reducing a degree of freedom and keeping $\theta_3 = 0$ all the time. In addition, the two swing angles are assumed to be constant in a Pseudo-Dynamic Stability Analysis. This means that when the suspension cables are deflected, they remain fixed in the deflected position as if the cable is a rigid body.

More assumptions are made to further simplify calculations: the time-dependent centripetal and gravitational forces derived from the pendulum swing are considered time-invariant constant forces, in addition to the inertia forces acting on the crane at its center of mass, which are considered constant as well. Also, payload damping was ignored (frictionless pivot and no air drag). Thus, it is obvious that this pseudo-dynamic

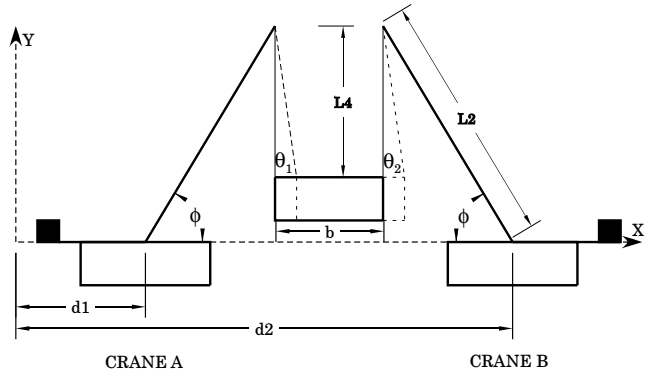

Fig. 5. Geometric constraints governing tandem lifting under straight-base motion.

estimation method does not study the full dynamics of the payload swing.

However, a comparison between the full dynamic analysis method and this type of suggested pseudo-dynamic estimation method was performed twice before in [19] and [20]. The torque caused by the weight and swing of the payload about the boom angle was calculated for both radial and tangential swinging directions using both approaches. It turned out that the error between the two torque values was insignificant for a realistic range of swing angles.

Nevertheless, to make the analysis more inclusive, the magnitude of the maximum swing angle is computed and applied to the model. This corresponds to the worst-case scenario when the payload swings most aggressively and compromises the crane's tip-over stability.

Finally, it should be noted that the swing deflection reduces the crane's tip-over stability because it moves the payload mass outwards, increasing the moment arm of the payload about the tip-over axis. The outward swing also induces a horizontal force at the tip of the boom. This force acts through the very long boom lever arm to create a large tipping moment. The fact that the payload is connected to both cranes makes the system more critical. Thus, it is important to reduce these oscillations as much as possible to maintain stability.

A. Straight-base Motion

The simplest motion of a crawler crane is driving both crane bases from one point to another, along a straight line, under a constant acceleration and a limited maximum speed. This is illustrated in Fig. 5. Vectors $\vec{d_1}$ and $\vec{d_2}$ represent the displacements of Crane A and Crane B respectively, with respect to a reference point.

Kane's method [21] is used to derive the equation of motion describing the swing angle θ_1. The second swing angle θ_2 is derived based on the geometric constraint equations.

The geometric constraint equations are expressed by:

$$d_1 + L_2\cos\phi_1 + L_4\sin\theta_1 + b - L_4\sin\theta_2 + L_2\cos\phi_2 - d_2 = 0 \quad (7)$$

$$L_2\sin\phi_1 - L_4\cos\theta_1 + L_4\cos\theta_2 - L_2\sin\phi_2 = 0 \quad (8)$$

To derive the equation of motion using Kane's method, we chose the generalized speed to be $u_1 = \dot{\theta}_1$. The velocity of the center of gravity of the payload B, with respect to the Newtonian reference frame, is expressed by:

$${}^N\vec{v}^B = \dot{d}_1\hat{i} + u_1\hat{k} \times L_4(\sin\theta_1\hat{i} - \cos\theta_1\hat{j}) \quad (9)$$

Because we have one generalized speed, then the expression for the first partial velocity is given by:

$${}^N\vec{v}_1^B = L_4(\sin\theta_1\hat{j} + \cos\theta_1\hat{i}) \quad (10)$$

To obtain the acceleration equation of the center of gravity of the payload, we differentiate (9) with respect to time to get:

$${}^N\vec{a}^B = \ddot{d}_1\hat{i} + \dot{u}_1L_4(\sin\theta_1\hat{j} + \cos\theta_1\hat{i}) + u_1^2L_4(\cos\theta_1\hat{j} - \sin\theta_1\hat{i}) \quad (11)$$

Kane's equations of motion are stated in terms of generalized inertia forces and generalized active forces [21]. The first generalized inertia force is given by:

$$F_1^* = -\frac{W}{g}{}^N\vec{a}^B \cdot {}^N\vec{v}_1^B \quad (12)$$

And the first generalized action force is given by:

$$F_1 = -W\hat{j} \cdot {}^N\vec{v}_1^B \quad (13)$$

Kane's equation of motion is formed by adding the generalized inertia and action forces and setting them to zero:

$$F_1^* + F_1 = 0 \quad (14)$$

$$m_4L_4\cos\theta_1(\ddot{d}_1 + \ddot{\theta}_1L_4\cos\theta_1 - \dot{\theta}_1^2L_4\sin\theta_1) + m_4L_4\sin\theta_1(\ddot{\theta}_1L_4\sin\theta_1 + \dot{\theta}_1^2L_4\cos\theta_1) = -m_4gL_4\sin\theta_1 \quad (15)$$

Because the swing angle should always be kept within a small range to avoid forward tip-over, and as the swinging motion happens at a very low speed, then we can linearize (15). Linearization is achieved by applying the small angle approximation for θ_1, i.e. $\sin\theta_1 = \theta_1$ and $\cos\theta_1 = 1$, and by eliminating all products of θ_1 and its derivatives. Thus, the linear differential equation is expressed by:

$$\ddot{\theta}_1(t) + \frac{g}{L_4}\theta_1(t) = -\frac{1}{L_4}\ddot{d}_1(t) \quad (16)$$

Solving (16) for θ_1 and using the results to obtain the values of θ_2 depending on the geometric constraint equations expressed in (7) and (8) will help predict what the crane system's response will be to different acceleration commands.

Defining $\ddot{d}_1 = a_1(t)$ and $\frac{g}{L_4} = \omega_n^2$, (16) can be expressed as:

$$\ddot{\theta}_1(t) + \omega_n^2\theta_1(t) = -\frac{1}{L_4}a_1(t) \quad (17)$$

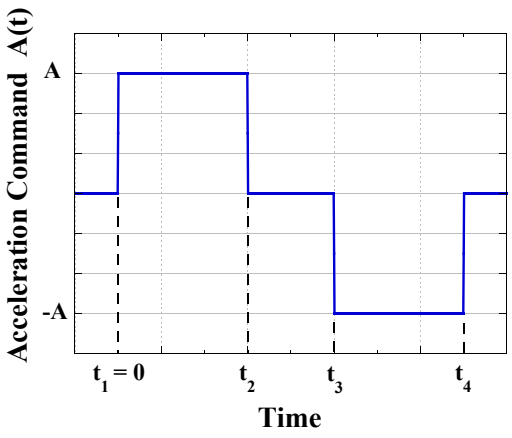

Fig. 6. Bang-coast-bang acceleration command.

Taking the Laplace Transformation of (17) gives:

$$s^2\Theta_1(s) + \omega_n^2\Theta_1(s) = -\frac{A(s)}{L_4} \tag{18}$$

Rearranging the equation, the transfer function of the system can be expressed as:

$$G(s) = \frac{\Theta_1(s)}{A(s)} = \frac{-1}{L_4(s^2+\omega_n^2)} \tag{19}$$

The time optimal command with a limited velocity and acceleration is a bang-coast-bang command, as shown in Fig. 6. This command profile is used as an input to move the base of Crane A in a point-to-point motion. A similar command is use to drive Crane B, $a_2(t) = \ddot{d}_2(t)$.

The bang-coast-bang command can be described as an acceleration step command with a magnitude A that consists of four steps; two positive and two negative. The bang-coast-bang command creates a trapezoidal velocity profile. In the Laplace domain, the command can be expressed as:

$$A(s) = \frac{A}{s}(1 - e^{-t_2 s} - e^{-t_3 s} + e^{-t_4 s}) \tag{20}$$

where A is the magnitude of the acceleration input and t_i is the corresponding timing of the i^{th} step in the command.

Now, to find a solution for the payload swing angle θ_1, the acceleration expression in the Laplace domain expressed in (20) is substituted in the transfer function expressed in (19). The resulting expression for $\Theta_1(s)$ is then transformed back into the time domain to get:

$$\theta_1(t) = \frac{-A}{L_4\omega_n^2}\Big(\big(1-\cos\omega_n t\big) - \big(1-\cos\omega_n(t-t_2)\big)\sigma(t-t_2) - \big(1-\cos\omega_n(t-t_3)\big)\sigma(t-t_3) + \big(1-\cos\omega_n(t-t_4)\big)\sigma(t-t_4)\Big) \tag{21}$$

It can be inferred from (21) that the maximum swing angle occurs when all four cosine terms are in phase, and the multiplying step functions σ are all equal to 1.

Finally, the values of θ_1 are used to calculate the values of θ_2 depending on the geometric constraints using:

$$\sin\theta_2 = \frac{1}{L_4}(d_1 + 2L_2\cos\phi + L\sin\theta_1 + b - d_2) \tag{22}$$

$$\cos\theta_2 = \cos\theta_1 \tag{23}$$

Assume that the two cranes' parameters are the same, and that the hoist cables have equal lengths, thus the payload stays level. As long as the acceleration commands acting on both cranes are synchronized, the two swing angles will be equal. A problem occurs if one of the cranes moves faster or slower than the other. In such cases, the geometry may cause one of the swing angles to increase dramatically and cause the whole system to collapse.

IV. Case Study

The derived equations were examined using the Kobelco 7250 as a case study. Two identical Kobelco cranes are assumed to be lifting a shared payload. The crane configuration used has no mast and a fixed-position counterweight was used for simplicity. The parameters of the Kobelco crane in this configuration are listed in Table I.

TABLE I. Parameters of the Kobelco 7250 [22].

Parameter	Item	Numerical Data
w	Width of base	7.47 m
h	Height of base	2.525 m
L_1	Length of base	8.97 m
L_2	Length of boom	70 m
L_3	Length of counterweight	5.85 m
L_4	Length of hoist	50 m
m_1	Mass of base	20 t
m_2	Mass of boom	20 t
m_3	Mass of counterweight	97 t
m_4	Mass of payload	64 t

A. Dynamic Analysis of Straight Line Motion of the Cranes' Bases

When the bases of the two cranes in tandem lifting move in a straight line under the effect of the bang-coast-bang acceleration command discussed previously, it induces residual swings of the payload as the crane bases come to a stop. Two major factors affect the value of the swinging angle of the payload: the total distance traveled by the crane base, and the width of the two pulses in the acceleration command.

For our case study, the maximum rated linear velocity of the crane base according to the data sheet is 1.1 km/h. So, it is assumed that the crane reaches this maximum speed within 1 s to account for the worst-case scenario, and this acceleration value is used as the amplitude of the bang-coast-bang command.

For a hoist length of 50 m, the period of oscillation is 14.18 s. Thus, the bang-coast-bang command creating the largest swing angle should last for twice that period. Changing

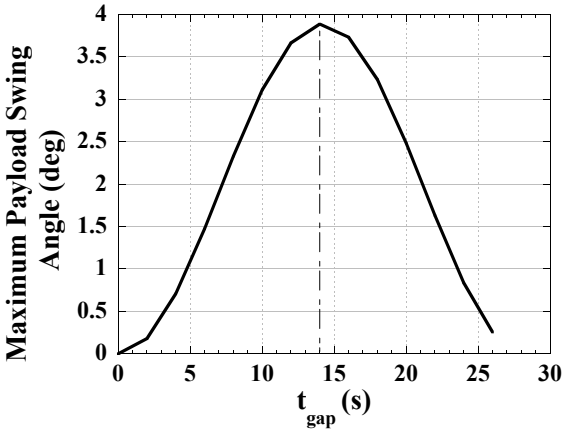

Fig. 7. Maximum payload swing angle in bang-coast-bang motion vs. t_{gap} with different acceleration durations.

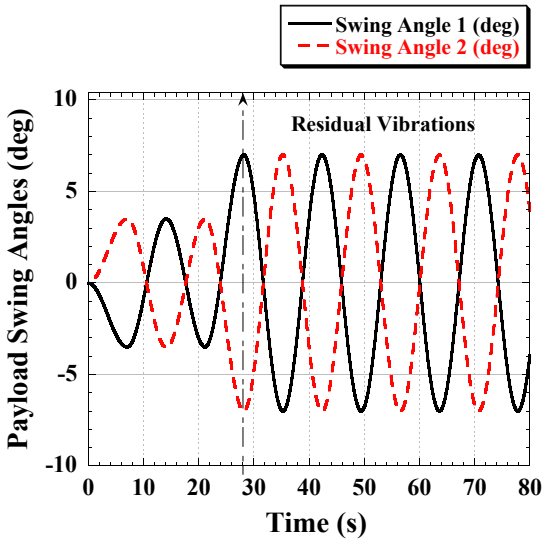

Fig. 8. Payload swing response of the two cranes to a bang-coast-bang acceleration command vs. Time (Maximum Oscillation).

the width of the acceleration and deceleration pulses, and consequently changing t_{gap}, results in different amplitudes for the payload's residual swing.

Fig. 7 shows the maximum payload swing with respect to t_{gap}. It can be inferred from the graph that the largest swing angle occurs when t_{gap} is equal to the period of oscillation of the payload; i.e. $t_{gap} = 14.18\ s$.

The response for two identical acceleration commands acting on the two cranes and creating maximum oscillations are shown in Fig. 8. The maximum swing angles in this case are identical and equal to 14^o peak-to-peak.

Because both the crane base movement and the payload swinging are slow movements, the payload was assumed to be positioned at the maximum swing angle mentioned above. In addition, the inertial force was added to the gravitational forces and forward tip-over stability analysis was performed based on the equations derived previously.

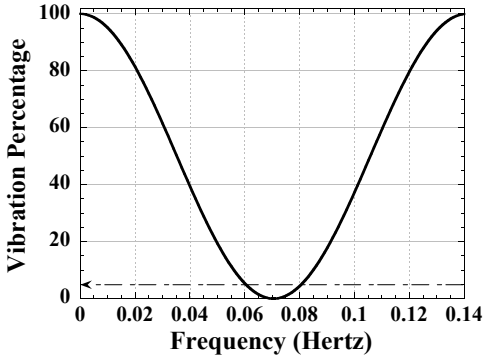

Fig. 9. Sensitivity curve of the ZVD shaper.

Results for a payload mass of 64 $t$show that a swing angle of 7^o is not large enough to create a forward tip-over moment. However, if the swing angle exceeds 11^o for a boom angle of 70^o, then the forward tip-over moment will be large enough to cause the whole system to collapse. To stay on the safe side, a command shaper is used for the two acceleration commands to minimize the payload residual oscillations. Note that larger payload masses would directly reduce the allowable swing out angle.

Input shapers usually satisfy a set of constraint equations while minimizing a performance criterion. In this case, the goal is to minimize the residual swing of the payload. For a system with one mode of vibration, with a natural frequency of ω_n, and a damping ratio of ζ, the percentage vibration is given by [14]:

$$V(\omega_n, \zeta) = e^{-\zeta\omega_n t_n}\sqrt{[C(\omega_n, \zeta)]^2 + [S(\omega_n, \zeta]^2} \qquad (24)$$

where,

$$C(\omega_n, \zeta) = \sum_{i=1}^{n} A_i e^{\zeta\omega_n t_i}\cos(\omega_n\sqrt{1-\zeta^2}t_i) \qquad (25)$$

$$S(\omega_n, \zeta) = \sum_{i=1}^{n} A_i e^{\zeta\omega_n t_i}\sin(\omega_n\sqrt{1-\zeta^2}t_i) \qquad (26)$$

A_i and t_i represent the amplitudes of the impulses and their time locations, and n is the number of impulses in the input shaper. These impulses are to be convoluted with the bang-coast-bang acceleration command applied to each of the cranes, to ensure minimum residual vibrations. Differentiating (24) with respect to time, setting it to zero, and solving for the amplitudes and time locations of the impulses results in the design of a ZVD shaper which is considered a robust shaper that limits the residual vibrations for a considerable range of natural frequencies, i.e. for a range of hoist lengths (approximately 40 - 70 m in our case). This can be seen in the ZVD sensitivity curve shown in Fig. 9.

For a natural frequency of $0.443\ rad/s$ and a damping ratio of 0, the amplitudes and time locations of our input shaper are as follows:

$$\begin{bmatrix} A_i \\ t_i \end{bmatrix} = \begin{bmatrix} 0.25 & 0.50 & 0.25 \\ 0 & 7.0925 & 14.1850 \end{bmatrix} i = 1, 2, 3 \qquad (27)$$

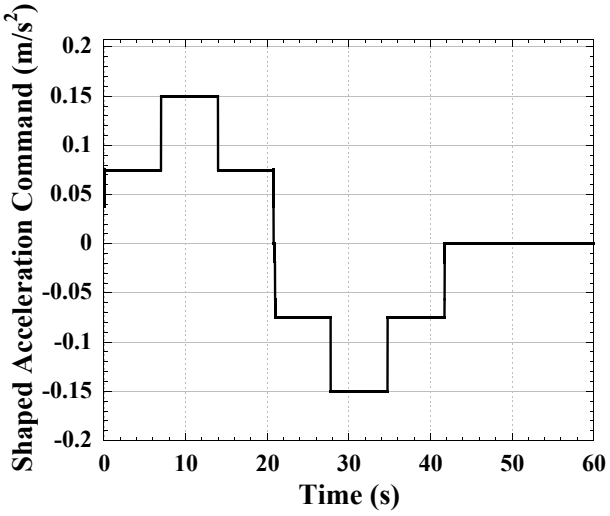

Fig. 10. Shaped acceleration command.

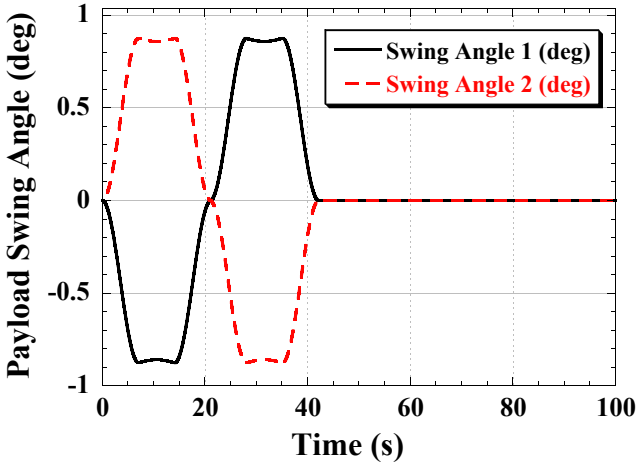

Fig. 11. Payload swing response of the two cranes to the shaped acceleration command vs. Time.

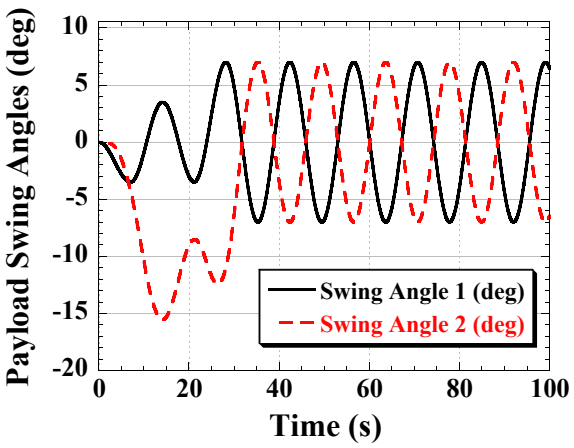

Fig. 12. Payload swing response of the two cranes to unsynchronized bang-coast-bang acceleration commands vs. Time.

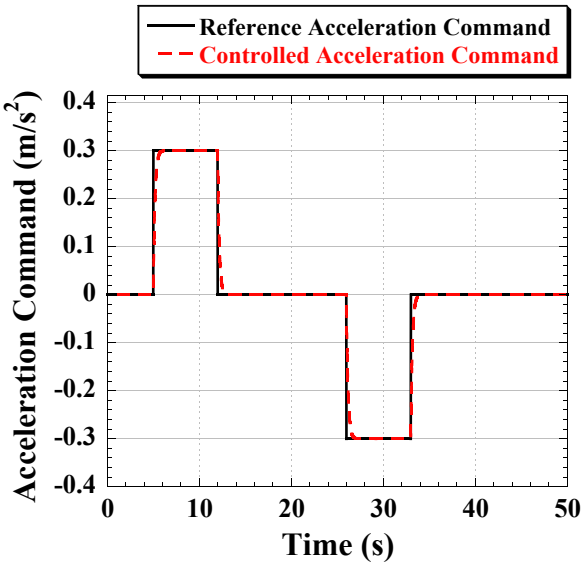

Fig. 13. Reference and controlled acceleration commands.

Convoluting the derived ZVD shaper with the bang-coast-bang acceleration command results in the signal shown in Fig. 10. Applying this shaped command to both crane bases, in perfect synchronization, gives the response shown in Fig. 11. It is clear that the shaper was able to eliminate the residual swing. The only cost for this improvement is that the system moves slightly slower. This is not crucial in this application, as safety is far more important than speed in crane operations.

As previously mentioned, the operation of both cranes needs to be perfectly synchronized. Fig. 12 shows what happens to the values of swing angles of both cranes if crane B was actuated 5 s later than Crane A. The figure shows that residual vibrations are not affected. However, it is noted that θ_2 reaches a value of 15^o at some point. This will definitely cause the system to collapse (The negative value of θ_2 represents the outward swinging of the payload away from crane B).

To tackle this problem, an integral controller was designed where a sensor monitors the motion of one crane, and an actuator is used to keep the motion of the other crane synchronized with the first one.

The integral controller was designed using Simulink, and it has a gain of 5.75. It reads the acceleration command given to crane A, and applies a similar command to crane B. Fig. 13 shows the reference command and the controlled command.

Thus, applying both the command shaper to minimize residual swing, together with the I-controller to synchronize the motion of both cranes guarantees safe operation during tandem lifting.

V. Discussion

Tandem lifting cranes are useful for moving heavy and bulky payloads. However, having two cranes connected by a shared payload makes the system more complicated and subject to greater tip-over hazard. The configuration and motions of the first crane directly affects the second crane. This complication provides additional factors that can cause tip-over accidents.

This paper presented some guidelines to ensure safety in tandem lifting. It analyzed the behavior of such a system when the cranes are moved in a straight line, and it presented an effective command shaper to minimize the swing of payloads in tandem lifting.

A controller was developed to synchronize the motion of the two cranes and eliminate the need for a second operator, thus minimizing the human error factor. This shaper and controller, along with additional sensors and monitoring devices could be employed to ensure safe operating conditions throughout the lift.

VI. Future Work

The results and insights obtained in this paper build a foundation for further work in the area of control of robotic crawler cranes. Future investigations can extend the analysis in several directions.

First, the pseudo-dynamic stability analysis can be improved to include more motion scenarios than the one discussed, such as boom luffing or hoisting. Combinations of these motions can also be studied. Another avenue of research is applying trajectory planning. This can guarantee optimum operation time, and will improve the quality of the lifting operation.

In addition, this paper only covered the analysis related to two identical cranes with identical parameters. In real applications, this is not usually the case. Differences in crane parameters should be taken into consideration. More than two cranes lifting a common load can also be considered.

Finally, follow-on research can consider crawler cranes in tandem lifting with movable counterweights. This will introduce interesting static and dynamic characteristics, which can improve the area of tip-over stability analysis of crawler cranes.

References

[1] Gottwald. (2007) Gottwald port technology: Safe solutions for lifting project cargoes. [Online]. Available: http://www.porttechnology.org/

[2] R. Kaibni. (2016) Pre-cast concrete yards: Safety and health management. [Online]. Available: https://www.projectmanagement.com/articles/314087/Pre-Cast-Concrete-Yards–Safety-and-Health-Management

[3] Vertikal. (2015) Seven gmk 6300l western australia. [Online]. Available: http://www.vertikal.net/en/news/story/17539/

[4] R. L. Neitzel, N. S. Seixas, and K. K. Ren, "A review of crane safety in the construction industry," *Applied Occupational and Environmental Hygiene*, vol. 16, no. 12, pp. 1106–1117, 2001.

[5] A. Rauch, W. Singhose, D. Fujioka, and T. Jones, "Tip-over stability analysis of mobile boom cranes with swinging payloads," *ASME Journal of Dynamic Systems, Measurement, and Control*, vol. 135, no. 3, pp. 031 008–1–6, 2013.

[6] K. L. Sorensen, W. Singhose, and S. Dickerson, "A controller enabling precise positioning and sway reduction in bridge and gantry cranes," *Control Engineering Practice*, vol. 15, no. 7, pp. 825–837, 2007.

[7] Z. N. Masoud and K. A. Alhazza, "Frequency-modulation input shaping control of double-pendulum overhead cranes," *ASME Journal of Dynamic Systems, Measurement, and Control*, vol. 136, no. 2, pp. 1–11, 2014.

[8] M. F. Daqaq, Z. N. Masoud, and A. H. Nayfeh, "Nonlinear modeling and control of quay-side container cranes," in *IMAC-XXIII: Conference and Exposition on Structural Dynamics*, Orlando, FL, 2005.

[9] M. F. Daqaq and Z. N. Masoud, "Nonlinear input-shaping controller for quay-side container cranes," *Nonlinear Dynamics*, vol. 24, no. 1, 2006.

[10] H. Liu, W. Cheng, and J. Jyi, "Cranes spreader dynamics research based on triangle flexible anti-swing system," *China Railway Science*, vol. 36, no. 2, pp. 103–110, 2015.

[11] E. M. Abdel-Rahman and A. H. Nayfeh, "Pendulation reduction in boom cranes using cable length manipulation," *Nonlinear Dynamics*, vol. 27, no. 3, pp. 255–269, 2002.

[12] M. J. Agostini, G. G. Parker, E. E. Kruse, H. Schaub, K. Groom, and R. D. Robinett, "Multiple axis boom crane maneuver generation for payload swing suppression," in *American Control Conference, 2001*, vol. 1, Arlington, VA, 2001, pp. 287–292.

[13] G. Parker, M. Graziano, F. Leban, J. Green, and J. Bird, "Reducing crane payload swing using a rider block tagline control system," in *OCEANS 2007-Europe*, Aberdeen, Scotland, UK, 2007, pp. 1–5.

[14] N. Singer, W. Singhose, and E. Kriikku, "An input shaping controller enabling cranes to move without sway," in *Seventh Topical Meeting on Robotics and Remote Systems*, Augusta, GA, 1997.

[15] B. Shinde, "Current status and key issues of automated robotic crane for various industrial applications," *International Journal of Recent Technology and Engineering*, vol. 2(5), November, 2013.

[16] K. S. Saidi, A. M. Lytle, and N. A. Scott, "Developments toward an autonomous robotic crane for automated steel construction," in *The* 11^{th} *Mediterrenean Conference on Control and Automation*, Rhodes, GR, 2003.

[17] S. Kang and E. Miranda, "Planning and visualization for automated robotic crane erection process in construction," *Automation in Construction*, vol. 15, pp. 398–414, 2006.

[18] Y. Li, X. Xi, J. Xie, and C. Liu, "Study and implementation of a cooperative hoisting for two crawler cranes," *Journal of Intelligent and Robotic Systems*, vol. 83, pp. 165–178, Nov. 6, 2015.

[19] D. Fujioka, "Tip-over stability analysis for mobile boom cranes with single- and double-pendulum payloads," Master's thesis, Georgia Institute of Technology, Atlanta, GA, 2010.

[20] A. Rauch, "Stability analysis of mobile boom cranes," Master's thesis, Georgia Institute of Technology, Atlanta, GA, 2008.

[21] A. K. Banerjee, *Flexible Multibody Dynamics: Efficient Formulations and Applications*. John Wiley and Sons, Ltd, 2016.

[22] Kobelco. Hydraulic crawler cranes(conventional model) 7250. [Online]. Available: http://www.kobelco-cranes.com/en/products/